Effect of Formic Acid As A Dopant in Tuning The Physical Properties of L-Arginine Acetate

*P. V. Radhika,** K. Jayakumari, ***C. K. Mahadevan
*Department of Physics, Lekshmipuram College of Arts & Science, Neyyoor – 629 802, Tamil Nadu, India.
**Department of Physics, Sree Ayyappa College for Women, Chunkankadai – 629 003, Tamil Nadu, India.
***Physics Research Centre, S.T. Hindu College, Nagercoil – 629 002, Tamil Nadu, India.

Abstract **- L- arginine acetate is one of the most common amino acid derivative. Single crystals of L-arginine acetate (LAA), a nonlinear optical (NLO) material, have been grown by the free evaporation method and characterized chemically, structurally, thermally, optically, mechanically and electrically. Effect of formic acid as an impurity (added at different concentrations) on the properties of LAA has been investigated. X-ray diffraction analysis indicates the crystal system as monoclinic. The functional groups have been identified using Fourier transform infrared spectral analysis. The crystals are found to be thermally stable up to 191 °C. The UV-Vis spectral analysis shows that these crystals have wide transparency range in the entire visible region. Second harmonic generation measurement shows the NLO property. Microhardness measurement indicates that the grown crystals come under soft material category. Dielectric measurements were carried out at various temperatures ranging from 40-140 °C and with various frequencies ranging from 1 kHz to 100 kHz by the parallel plate capacitor method. The AC activation energies were also estimated. The low dielectric constant values observed for pure and doped LAA indicate that the crystals grown are not only promising NLO materials but also low dielectric constant value dielectric materials.**

Key words: L-arginine acetate, slow evaporation technique, doping effects.

INTRODUCTION

In the organic class, crystalline salts of amino acids are one of the directions for searching new NLO materials, which recently has attracted considerable interest. Amino acids and their complexes are promising materials for NLO applications as they contain a proton donor carboxyl acid (-COO) group and the proton acceptor amino (NH_2) group. L-arginine is an amino acid that forms a series of complexes upon reaction with different acids [1]. Following this, series of amino acid crystals such as L-arginine acetate (LAA) [2], L-arginine oxalate (LAO) [2], L-arginine hydrobromide (LAHBr) [3], L-arginine hydrochloride (LAHCl) [4], L_arginine diphosphate [5], L-arginine hydroflouride (LAHF) [6] and L-arginine dinitrate (LHDN) [7] were grown and characterised. These crystals were reported to have promising NLO properties comparable to that of the well-known inorganic crystal KDP. L-arginine acetate is a nonlinear optical material having a powder second harmonic generation (SHG) efficiency nearly three times that of KDP [8].

A considerable interest has been shown recently in studying the effect of impurities (both organic and inorganic) on the growth and properties of some hydrogen bonded crystals. Presence of impurity molecules, even at lower concentrations in the parent solute, may have considerable effect on the growth kinetics and other properties of LAA crystals as already reported by several research workers on their systems [8 - 13].

In the present work, we have made an attempt to grow hybrid material single crystals by doping LAA with formic acid taken at different concentrations and to investigate the effect of doping on the various properties of LAA crystals. Results obtained are reported herein.

2. EXPERIMENTAL

2.1 Crystal growth

Analytical Reagent (AR) grade L-arginine and acetic acid were taken in the equimolar ratio (1:1) and dissolved in doubly deionised water to synthesize LAA according to the reaction

$(NH_2)NHCNH(CH_2)_3CH(NH_2)COOH + CH_3COOH \rightarrow (NH)_2^+CNH(CH_2)_3CH(NH_3)^+COO^-CH_3COO^-$

The solution was stirred well at constant rate to get homogeneity. The solution was transferred to a beaker and it was allowed to evaporate at room temperature for some days to get the undoped LAA crystals.

To obtain formic acid doped (at different concentrations, viz. 0.2, 0.4, 0.6 and 0.8 mol%) LAA single crystals, required amount of formic acid (in each case) was added to the solution of pure LAA and similar procedure adopted for the growth of pure LAA crystal was followed. Pure and doped LAA crystals with a significant size could be grown within a period of 15-20 days. Good quality single crystals were obtained when the pH value was

within 5 and 6. The single crystals grown in the present study are represented as LAA(pure LAA), LAAF1(0.2 mol% doped), LAAF2(0.4 mol% doped), LAAF3(0.6 mol% doped) and LAAF4(0.8 mol% doped).

2.2 Characterizations

Densities of the grown crystals were measured by the floatation method with a mixture of carbon tetra chloride (density-1.592 g/cc) and hexane (0.652 g/cc) taken as high and low density liquids respectively.

CHNS analysis was carried out using an Elementar Vario EL III to estimate the carbon, hydrogen and nitrogen atom contents in the grown crystals.

The grown crystals were subjected to single crystal X- ray diffraction (SXRD) study using an ENRAF – NONIUS CAD4 single crystal X–Ray diffractometer. Powder X-Ray diffraction (PXRD) analysis was also carried out to understand the crystallinity of the grown crystals using an XPERT-PRO diffractometer with monochromated CuK_α radiation (λ =1.54056 AU). The reflections were indexed following the procedure of Lipson and Steeple [14].

FTIR spectra were recorded in the mid-infrared region (wavenumber range 400-4000 cm^{-1}) using a MAGNA 550 model spectrometer. In order to understand the optically transparent nature of the grown crystals, UV-Vis absorption spectra were recorded in the wavelength range 200-800 nm using a Vario Cary 500 scan spectrophotometer.

SHG measurements were made on the grown crystals using a 1064 nm Quanta ray laser and a Molectron powermeter.

Thermal study(TGA, DTA and DSC analyses) was carried out for LAA and LAAF4 using a SDT Q600 V8.3 Build 101 analyser in a temperature range of room temperature to 800 °C in air atmosphere to understand the thermal stability of the grown crystals.

Mehanical strength of the grown crystals were studied by measuring the microhardness on the large area face with the help of a Leitz microhardness tester.

The capacitance (C_{crys}) and dielectric loss factor (tanδ) measurements were carried out to an accuracy of ±1 % on all the five grown crystals having the large area faces touching the electrodes by the parallel plate capacitor method [2] using an LCR meter (Agilant 4284A) at various temperatures ranging from 40-140 °C with three different frequencies, viz.1 kHz, 10 kHz, and 100 kHz. The temperature was controlled to an accuracy of ±1 °C. The observations were made while cooling the sample. The dimensions of the crystals were measured using a traveling microscope. Air capacitance (C_{air}) was also measured. Since the variation of air capacitance with temperature was found to be negligible, air capacitance was measured only at the lower temperature considered. The crystals were shaped and polished and the opposite faces were coated with graphite to form a good conductive surface layer (ohmic contact). The sample was mounted between the silver electrodes and annealed at 140 °C for about 30 min to homogenize the sample before taking the readings.

As the crystal area was smaller than the plate area of the cell, the real part of the dielectric constant ($\epsilon' = \varepsilon_r$) of the crystal was calculated using Mahadevan's formula [2,15]

$$\varepsilon' = \varepsilon_r = (Aair/Acrys)\ ((Ccrys - Cair)\ (1- Acrys/Aair))/Cair)$$

where C_{crys} is the capacitance with crystal (including air), C_{air} is the capacitance of air, A_{crys} is the area of the crystal touching the electrode and A_{air} is the area of the electrode.

The AC electrical conductivity, σ_{AC}, was calculated using the relation

$$\sigma_{AC} = \varepsilon_0 \varepsilon_r\, \omega \tan\delta$$

where ε_0 is the permittivity of free space ($8.85x10^{-12}$ $C^2N^{-1}m^{-2}$), ω is the angular frequency ($\omega = 2\pi f$; f=1, 10 and 100 kHz in the present study) and tanδ is the dielectric loss factor.

3. RESULTS AND DISCUSSION

3.1 Densities, lattice parameters and chemical composition

The crystals grown in the present study, both pure and doped LAA, are found to be colourless and transparent .The photographs of the sample crystals grown are shown in Figure 1. It is found that, as dopant concentration increases the transparency of the crystal increases.

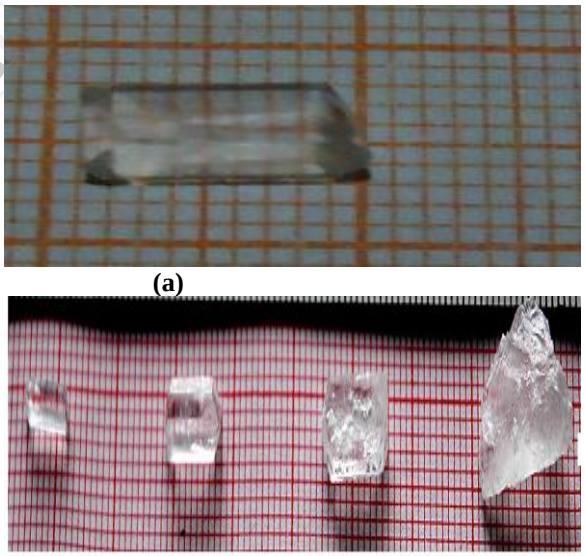

(a)

(b)

Figure 1: Photographs of the sample crystals grown - (a) LAA and (b) From right LAAF1, LAAF2, LAAF3 and LAAF4

The observed weight percentages of carbon, hydrogen and nitrogen present in both pure and doped LAA are provided in Table.1. Formic acid also contains C and H atoms. Variations in C, N and H concentrations observed are found to be insignificant. However, the results observed indicate that the basic material of the grown crystals is L-arginine acetate. This analysis is not sensitive enough to estimate the impurity concentration as the impurity concentration considered in the present study is very small.

Table 1: Chemical analysis of pure and formic acid doped LAA

Crystal	Composition (%)		
	C	H	N
LAA	40.98	12.82	24.52
LAAF1	40.85	12.89	24.30
LAAF2	40.86	12.52	24.40
LAAF3	40.82	12.32	24.16
LAAF4	40.84	12.48	24.40

Results obtained from density and SXRD measurements are provided in Table 2. The measured density is found to increase with the increase in impurity concentration indicating that the impurity molecules have entered into the LAA crystal matrix. The observed variation in lattice volume also endorses this. Lattice parameters observed in the present study for the pure LAA crystal compare well with those reported in the literature [12].

The PXRD patterns observed in the present study are shown in Figure 2. The sharp peaks observed indicate the higher crystalline nature of the grown crystals. The observed patterns confirm the material of the grown crystals as basically LAA [12].

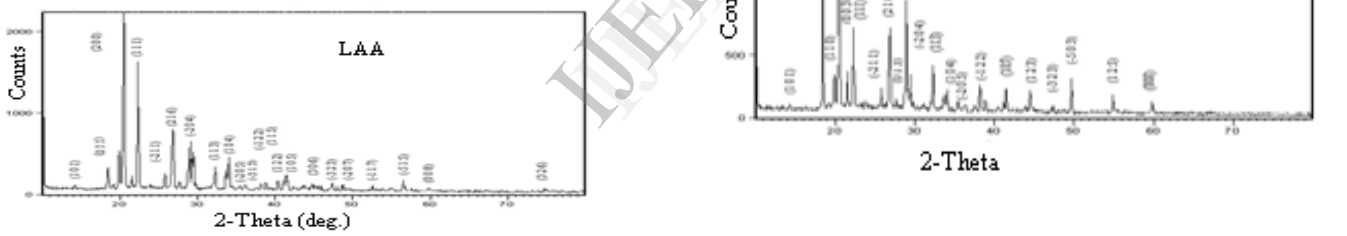

Figure 2: The observed PXRD patterns

Table 2: Single crystal XRD data for pure and formic acid doped LAA crystals

Crystal	Lattice parameters							Crystal system	Space group	Density (g/cc)
	a (Å)	b (Å)	c (Å)	A(°)	B(°)	Γ(°)	Volume (Å^3)			
LAA	9.189 (9.174)	5.166 (5.172)	13.050 (13.478)	90	109.6 (110.1)	90	584.0 (600.4)	Monoclinic	$P2_1$	1.323
LAAF1	9.220	5.178	13.110	90	109.7	90	590.0		$P2_1$	1.366
LAAF2	9.226	5.168	13.077	90	109.6	90	587.0	Monoclinic	$P2_1$	1.367
LAAF3	9.207	5.173	13.080	90	109.0	90	587.2	Monoclinic	$P2_1$	1.449
LAAF4	9.205	5.173	13.079	90	109.5	90	587.3	Monoclinic	$P2_1$	1.469

Reported values are given in parenthesis [12]

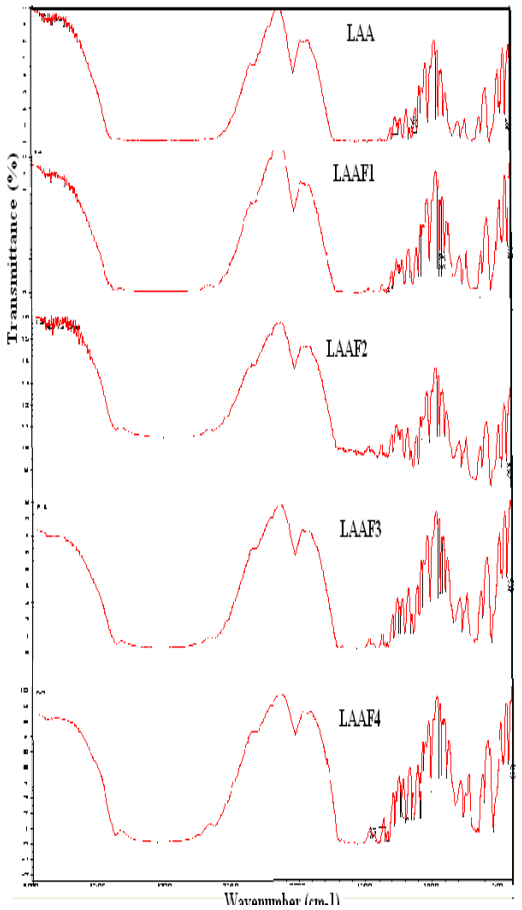

Figure 3: The observed FTIR spectra

The FTIR spectra recorded in the present study for pure and doped LAA crystals are shown in Figure 3. The spectra are found to be complex as a result of various functional groups present in the pure and doped LAA crystals. The vibrational band assignments are given in Table 3.

Both the pure and doped LAA crystals show a broad envelope between 2100-3500 cm^{-1}. It is due to overlapping of peaks of NH (NH^{3+}), OH (COOH) and CH (CH_2 and CH_3) vibrations. The absorptions at around 3750-2300 cm^{-1} show the presence of NH and CH stretching vibrations. The peak observed at around 2025 cm^{-1} is for symmetrical NH^{3+} bending. The spectrum of LAA shows a strong stretching absorption near 1550 cm^{-1} which is the characteristic of acyclic –NH stretching and –OH stretching. All other peaks below 1440 cm^{-1} are due to COO^- and other bending modes. The peak, due to torsional NH oscillations of NH_3^+ is observed at 543 cm^{-1}[13].

FTIR spectra of doped crystals are almost similar to that of pure LAA crystal. However, a significant change in absorption level is seen due to stretching modes, in between the band ranging from 1600 to 1200 cm^{-1}, when the doping concentration is increased. From these variations, we can understand the dopant inclusion into the LAA crystal matrix.

Table 3: The vibrational band assignments

LAA (Reported [8])(cm^{-1})	LAA (present work) (cm^{-1})	LAAF1 (cm^{-1})	LAAF2 (cm^{-1})	LAAF3 (cm^{-1})	LAAF4 (cm^{-1})	Assignment
3750-2300	3900-2300	3900-2300	3900-2300	3900-2300	3900-2300	3750-2300 NH and CH stretching vibrations
2025	2025.35	2025.75	2025.74	2025.93	2025.65	AsymmetricNH_3^+ bending
1532	1557.39	1560.11	1555.43	1556.04	1557.93	Asymmetric stretching modes of COO^-
			1395.79	1414.63	1399.87	CH_3 symmetric deformation
		1322.85	1322.85	1323.04	1356.10	Stretching vibration of CO
					1340.38	CH_3 wagging
					1323.18	CH_2 twisting
1228	1229.10	1228.94	1228.82	1229.06	1229.15	C-C-COO vibrations
1197	1197.02	1196.87	1196.22	1197.05	1197.13	-COO vibrations

1093	1089.74	1089.62	1089.56	1089.75	1089.75	C-CN stretching vibrations
928	928.93	928.94	928.88	928.98	928.89	C-CH bending
		914.91		915.09		Overtone of torsional oscillation of NH_3^+
670	675.87	671.32	653.46	671.39	653.16	NH out of plane bending

3.2 Thermal, optical and mechanical properties

The TGA, DTA and DSC patterns observed for LAA and LAAF4 are shown in Figure 4. It is observed that the decomposition of LAA starts at 204 ºC. This is supported by the results of DTA and DSC analyses where the endothermic reaction is observed at 202 ºC. It can be seen from the thermal analyses that LAA subjected to continuous heating does not remain stable for a long temperature change. However, it is decomposed at a temperature 582 ºC and forms a residue. Above 632 ºC, the product is stable without any prominent weight loss. LAAF4 starts decomposing at 191 ºC. Other decompositions observed for LAAF4 are at temperatures 286, 457 and 587 ºC, and above 741 ºC there is no prominent weight loss observed.

Since there is no endothermic or exothermic transition below 200 ºC, the materials are proved to be stable in this region. The resistivity of the materials against thermal crack is evident as the DSC trace is smooth up to nearly 200 ºC. It is the property observed for compounds where the lattice force is more predominating than the covalent bonding forces in molecules. It is also observed that the electrostatic force that originated as a result of perfect proton transfer between acetic acid and L-arginine becomes dominating to provide resistance to melting before decomposition [16].

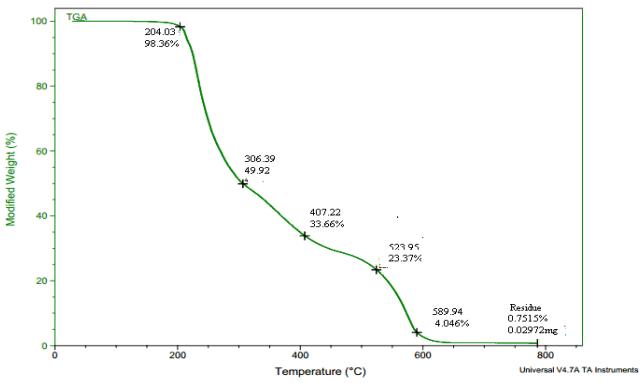

(a)

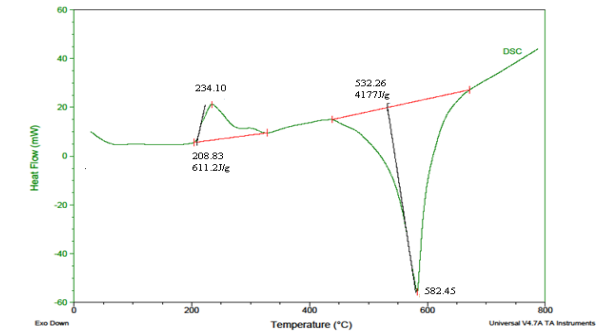

(b)

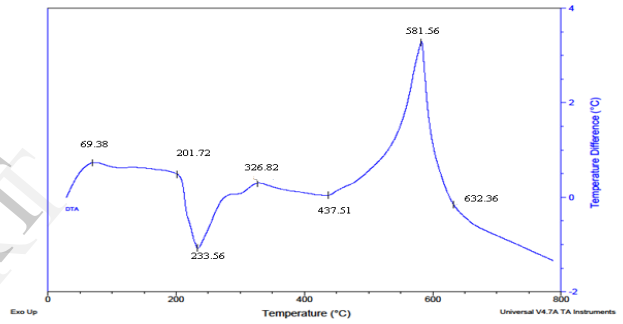

(c)

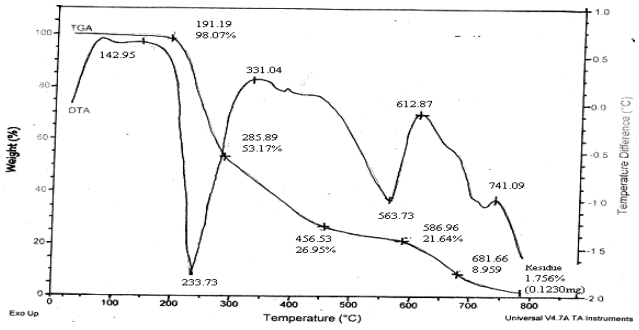

(d)

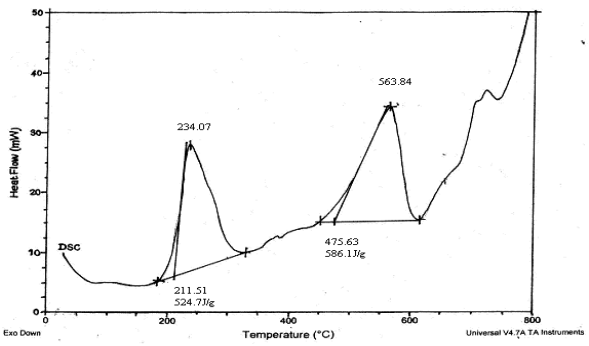

(e)

Figure 4: The observed TG, DTA and DSC

patterns [(a), (b) and (c) are respectively the TG, DTA and DSC patterns of LAA crystals; and (d) and (e) are respectively the TG/DTA and DSC patterns of LAAF4 crystal]

The range and percentage of optical transmission of pure and doped LAA crystals were studied by using the UV – Vis spectra of the grown crystals recorded in the wavelength range 200 – 800 nm. The spectra of pure and formic acid doped LAA observed in the present study are shown in Figure 5.

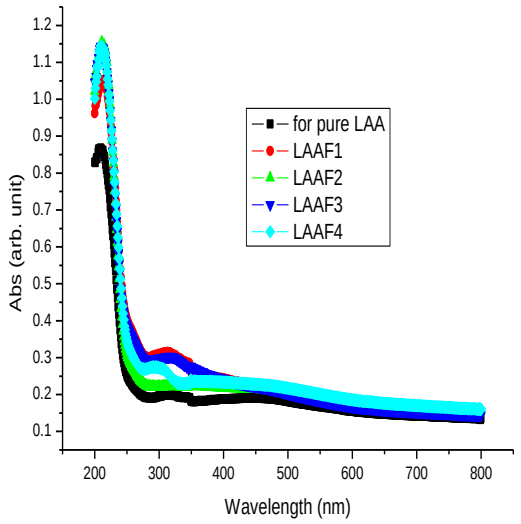

Figure 5: The observed UV-Vis absorption spectra

Table 4: The optical absorption edges, SHG efficiencies and work hardening coefficients observed in the present study

Crystal sample	Absorption edge(nm)	SHG efficiency(in urea unit)	Work hardening coefficient(n)
LAA	236.4	1.05	3.361
LAAF1	232.9	1.19	3.212
LAAF2	229.4	0.89	3.276
LAAF3	233.8	0.81	3.190
LAAF4	237.2	1.06	3.168

The optical absorption edges, SHG efficiencies and work hardening coefficients observed are provided in Table 4. It is observed that the lower cut off wavelength is around 236 nm, and the transparency conveniently extends to 800 nm.

SHG efficiency of the grown crystals was confirmed by adopting the Kurtz and Perry method. Urea crystal was used as the reference material in the SHG measurement. The SHG efficiencies observed for the grown crystals are found to be comparable to that of urea.

Hardness is defined as the resistance offered by a material to external mechanical action endeavouring to scratch, indent, or any other way affecting its structure. In the present study, microhardness measurements were carried out on all the five grown crystals using a Vicker's Hardness Indenter. Vicker's Hardness Number (H_V) was calculated using the relation

$$H_V = 1.8554P/d^2 \text{ kgmm}^{-2}$$

where P is the load applied and d is the diagonal length of the indented impression.

Figure 6 shows the plots between load P and hardness number H_V observed in the present study. Results obtained indicate that the hardness number increases with the increasing load for all the five crystals grown and characterized in the present study. Also, it is understood that doping decreases the Hardness but nonlinearly with the dopant concentration. The nonlinear variation due to dopant concentration may be understood as due to the randomness in formate of dopant replacing the acetate in LAA or in occupying the interstitials in LAA crystal matrix.

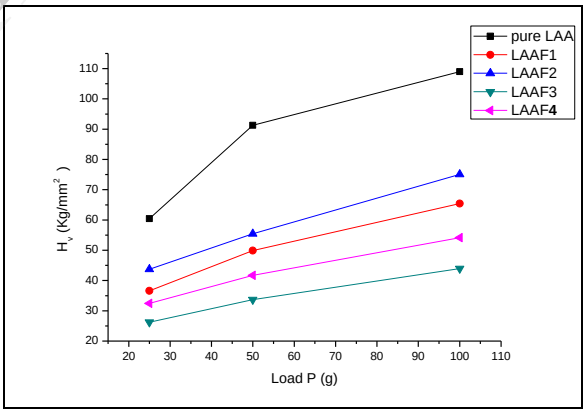

Figure 6: Variation of Vicker's hardness number with load for pure and doped LAA crystals

From Figure 6, it can be understood that the hardness number of the crystal increases with increasing load for both pure and doped samples. The work hardening coefficients 'n' for the pure and doped LAA crystals were estimated from the plots (not shown here) between logP and logd. If n>2, the microhardness number H_v increases with increasing load and if n<2, H_v decreases with increasing load [17]. Also, if n>1.6 the crystal is considered to be of soft materials category. Results obtained in the present study indicate that the crystals grown in the present study are of soft materials category. Also, the crystals exhibit the normal size indentation effect.

3.3 Electrical properties

The study of dielectric constant of a material gives an outline about the nature of atoms, ions and their bonding in the material. The dielectric parameters, viz. dielectric constants, dielectric loss factors and AC electrical conductivities observed in the present study for all the five crystals grown are shown respectively in Figures 7, 8 and 9. The AC activation energies (E_{AC}) were estimated by fitting the AC electrical conductivity data to the Arrhenius relation

$$\sigma_{AC} = \sigma_{AC0}\exp(-E_{AC}/(kT))$$

where σ_{AC0} is the material dependent constant, k is the Boltzmann constant and T is the absolute temperature. The estimated AC activation energies are given in Table 5.

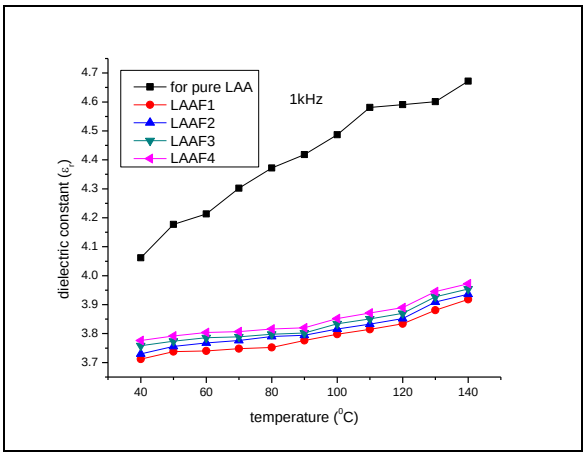

(a)

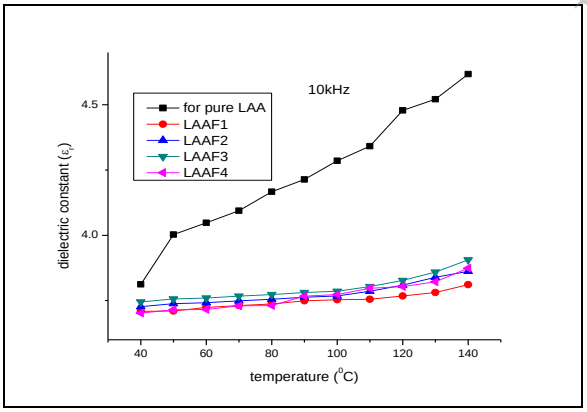

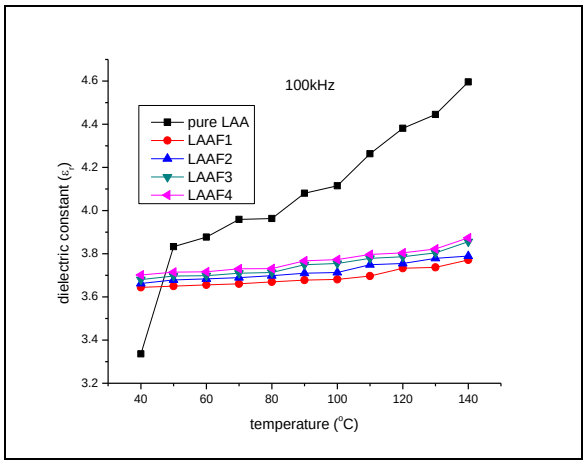

(b)

(c)

Figure 7: The observed dielectric constants

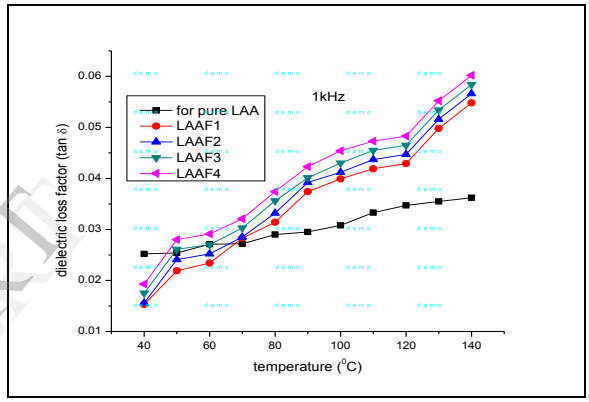

(a)

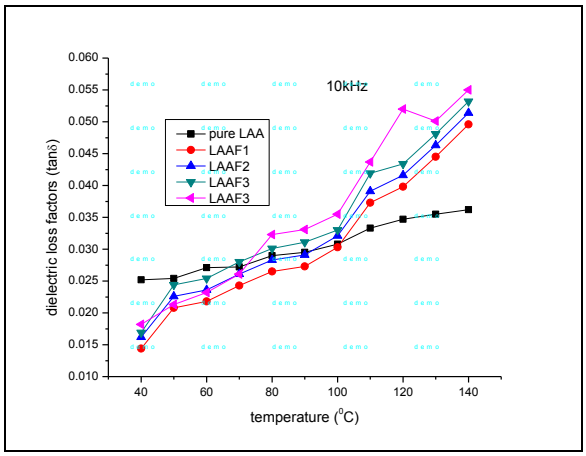

(b)

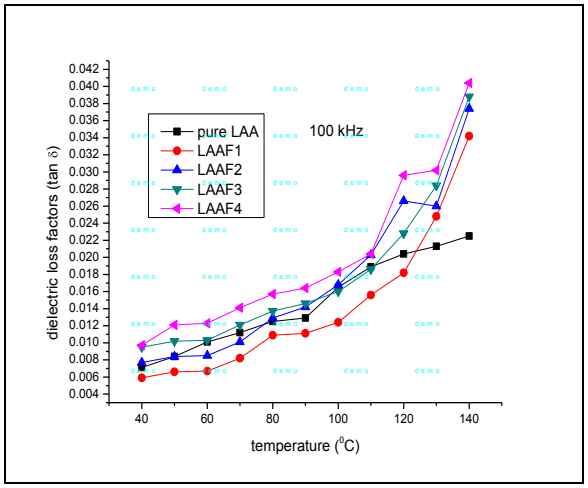

(c)

Figure 8: The observed dielectric loss factors

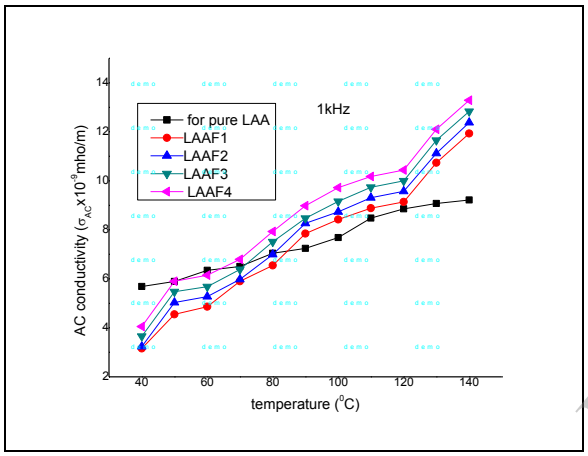

(a)

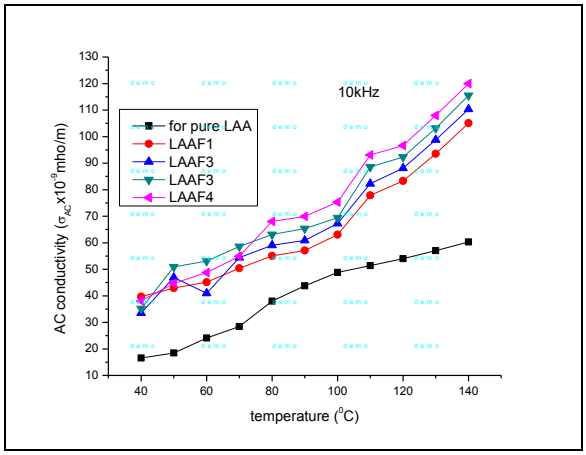

(b)

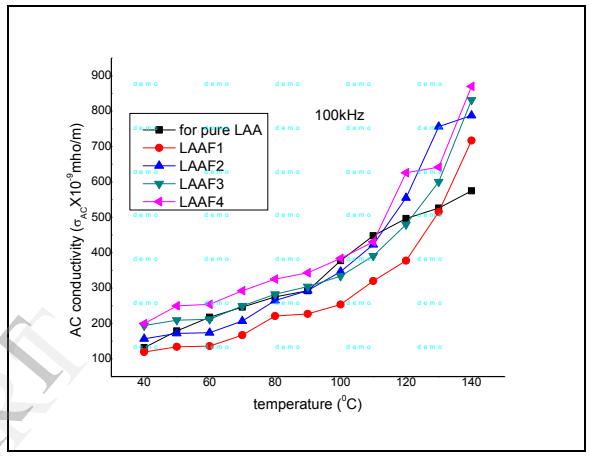

(c)

Figure 9: The observed AC electrical conductivities

All the three dielectric parameters considered are found to increase with the increase in temperature. Moreover, the ε_r and tanδ values are found to decrease whereas the σ_{AC} values are found to increase with the increase in frequency. This is a normal dielectric behaviour [2,12]. The dielectric loss factors observed are found to be low which indicates that the grown crystals are of high quality. The activation energy values observed are found to be less which indicates the presence of oxygen vacancies in the temperature range considered.

Table 5: The estimated AC activation energies

Crystal sample	AC activation energy, E_{AC}(eV) for frequencies		
	1 kHz	10 kHz	100 kHz
LAA	0.057	0.153	0.157
LAAF1	0.134	0.109	0.188
LAAF2	0.124	0.123	0.192
LAAF3	0.117	0.115	0.149
LAAF4	0.129	0.127	0.148

The low ε_r values observed for the pure LAA (at low temperature) and doped LAA crystals (at all temperatures considered) indicate that the crystals grown in the present study are not only potential NLO materials but also promising low ε_r value dielectric materials, expected to be useful in both the photonics and microelectronics industries [2]. Moreover, the doped LAA crystals can be considered to be more useful as they exhibit significantly less temperature dependent variation of dielectric constant. The present study, thus, indicates that doping with formic acid has tuned significantly the dielectric properties of LAA crystal.

Doping leads to decrease of dielectric constant significantly. However, the variation is found to be nonlinear with the dopant concentration. The other dielectric parameters also vary nonlinearly with the dopant concentration. This can be explained as due to the randomness in formate of dopant replacing the acetate in LAA and occupying the interstitials in the LAA crystal matrix.

CONCLUSIONS

Pure and formic acid doped LAA single crystals have been grown successfully by the slow evaporation method. SXRD measurements confirm that all the five (pure and four doped) grown crystals belong to the monoclinic crystal system. The PXRD patterns observed confirm the crystallinity. PXRD, FTIR spectral and CHNS elemental analyses indicate that LAA is the basic material of all the five crystals grown. The observed variations of density and lattice volume with doping concentration used for the growth of crystals indicate that the dopant molecules have entered into the LAA crystal matrix. Thermal analyses indicate that the grown crystals are thermally stable at least up to 191^{o}C. Results of optical, mechanical and electrical measurements indicate that doping with formic acid tunes these physical properties of LAA crystal significantly. Nonlinear variation of physical parameters observed with dopant concentration could be understood as due to the randomness in formate of dopant replacing the acetate in LAA and occupying the interstitials in the LAA crystal matrix. The present study indicates that the formic acid doped LAA crystals are not only potential NLO materials but also low ε_r value dielectric materials expected to be highly useful in photonics and microelectronics industries.

REFERENCES

1. X.J. Liu, Z.Y.Wang, X.Q. Wang, G,H. Zhang,S.X. Xu, A.D. Duan, S.J. Zhang, Z.H. Sun, and D. Xu (2008) *Cryst. Growth & Design 8(7),* 2270-2274.
2. M. Meena and C.K. Mahadevan (2008) *Materials Letters 62,* 3742-3744.
3. S. Mukerji and T. Kar (1998) *Mater. Chem. Phys. 57(1),* 72- 76.
4. L.N. Rashkovich and B.Yu. Shekunov(1991) *J.Cryst.Growth 112,* 183-191.
5. R. Ittyachan and P. Sagayaraj (2002) *J. Cryst. Growth 243*, 356-360.
6. J. Packiam Julius, S. A. Rajasekar, A. Joseph Arul Pragasam, V. Joseph and P.Sagayaraj (2004) *Mater. Sci. Engg. B 107*, 259-?.
7. P.C. Thomas, J. Thomas, J. Packiam Julius, J. Madhavan, A.Selvakumar and P.Sagayaraj (2005) *J. Cryst. Growth 277*, 308-313.
8. M. Gulam Mohamed, M. Vimalan, J.G.M. Jesudurai, J. Madhavan,and P. Sagayaraj(2007) *Cryst. Res. Technol. 42*, 948-954.
9. N. Kanagathara, G. Anbalagan, N.G. Renganathan (2011) *Int. J. Chem. Res. 1 (3),11-15.*
10. V. Natarajan, M. Arivanandhan,K.Sankaranarayanan, P. Ramasamy (2009) *J. Sci.Technol. 3(8) 897-899.*
11. P. Gnanasekaran, and J. Madahvan (2008) *Indian J. Sci.Technol. 1(7),* ?-? .
12. M.Meena and C.K.Mahadevan (2010) *Archieves of Applied Science Research 2(6),* 185-199.
13. P.V. Radhika, K. Jayakumari and C.K. Mahadevan (2013) *Int. J. Eng. Res. Appl. (IJERA) 3(6),* 1841-1849.
14. H. Lipson and H. Steeple (1970) *Interpretation of X-ray Powder Diffraction Patterns* [Macmillan, New York].
15. C.K.Mahadevan and K.Jeyakumari (2008) *Physica B : Condensed Matter 403*, 3990-3996.
16. S.E. Joema, S. Perumal, S. Ramalingam and P.Selvarajan (2011) *Recent Research in Science and Technology 3(3),* 63-68.
17. J.M. Kavitha and C.K.Mahadevan (2013) *Int. J. Eng. Res. Appl. (IJERA) 3(5),* 1931-1940.